ROYAL SOCIETY OPEN SCIENCE

royalsocietypublishing.org/journal/rsos

Research

Cite this article: Dearden RP, Johanson Z, O'Neill HL, Miles K, Bernard EL, Clark B, Underwood CJ, Rücklin M. 2025 Three-dimensional fossils of a Cretaceous collared carpet shark (Parascylliidae, Orectolobiformes) shed light on skeletal evolution in galeomorphs. *R. Soc. Open Sci.* **12**: 242011. https://doi.org/10.1098/rsos.242011

Received: 26 November 2024
Accepted: 17 March 2025

Subject Category:
Organismal and evolutionary biology

Subject Areas:
palaeontology, evolution

Keywords:
Elasmobranchii, Orectolobiformes, Galeomorphii, CT scanning, Cretaceous

Author for correspondence:
Richard P. Dearden
e-mail: richard.dearden@naturalis.nl

Electronic supplementary material is available online at https://doi.org/10.6084/m9.figshare.c.7778783.

THE ROYAL SOCIETY PUBLISHING

Three-dimensional fossils of a Cretaceous collared carpet shark (Parascylliidae, Orectolobiformes) shed light on skeletal evolution in galeomorphs

Richard P. Dearden[1,2], Zerina Johanson[3], Helen L. O'Neill[4], Kieran Miles[3], Emma L. Bernard[3], Brett Clark[3], Charlie J. Underwood[5] and Martin Rücklin[1]

[1]Vertebrate Evolution, Development, and Ecology, Naturalis Biodiversity Center, Leiden 2333 CR, The Netherlands
[2]School of Geography, Earth & Environmental Sciences, University of Birmingham, Birmingham, B15 2TT, UK
[3]Natural History Museum, London, SW7 5BD, UK
[4]CSIRO Australian National Fish Collection, National Research Collections Australia, Hobart, Tasmania TAS 7001, Australia
[5]School of Natural Sciences, Birkbeck College, London WC1E 7HX, UK

RPD, 0000-0003-3522-7304; ZJ, 0000-0002-8444-6776; HLO'N, 0000-0001-7096-687X; KM, 0009-0008-5294-1132; MR, 0000-0002-7254-837X

A rich fossil record of teeth shows that many living shark families' origins lie deep in the Mesozoic. Skeletal fossils of the sharks to whom these teeth belonged are far rarer and when they are preserved are often flattened, hindering understanding of the evolutionary radiation of living shark groups. Here we use computed tomography to describe two articulated Upper Cretaceous shark skeletons from the Chalk of the UK preserving three-dimensional neurocrania, visceral cartilages, pectoral skeletons and vertebrae. These fossils display skeletal anatomies characteristic of the Parascylliidae, a family of Orectolobiformes now endemic to Australia and the Indo Pacific. However, they differ in having a more heavily mineralized braincase and a tri-basal pectoral fin endoskeleton, while their teeth can be attributed to a new species of the problematic taxon *Pararhincodon*. Phylogenetic analysis of these new fossils confirms that *Pararhincodon* is a stem-group parascylliid, providing insight

into the evolution of parascylliids' distinctive anatomy during the late Mesozoic–Cenozoic shift in orectolobiform biodiversity from the Northern Atlantic to the Indo Pacific. Meanwhile both *Pararhincodon* and extant parascylliids have a distinctive vertebral morphology previously described only in Carcharhiniformes, contributing a skeletal perspective to the picture emerging from macroevolutionary analyses of coastal, small-bodied origins for galeomorphs.

1. Introduction

The evolutionary history of sharks (Selachii) is an emerging focus of macroevolutionary studies [1–3] but is obscured by a sparse record of skeletal fossils. Because of their high evolutionary distinctiveness [4] and diversity in form and habitat yet tractable size [5], sharks are increasingly used as a group in which to understand the interplay of phenotype, habitat and diversity through time [1–3], and are moreover important from an ecological and conservation perspective [6]. Underlying these studies is a rich fossil record of isolated teeth, which shows that the selachian crown-group stretches far back into the Mesozoic [7] and which are used to constrain the evolutionary history of the group in time. However, there is a limit to the information that teeth and their limited character sets can provide for estimates of phylogeny and evolutionary timing [8], and the cartilaginous skeletons of these early crown-group selachians, which would provide more information, have a low preservational potential. Even in those Mesozoic Fossil-Lagerstätten that do preserve potentially information-rich skeletons, these fossils are often flattened [9–13], making it difficult to extract the level of detailed three-dimensional skeletal data that has demystified much of the record of sharks' older, Palaeozoic relatives [14–16]. This restricts understanding of key phylogenetic problems at the roots of selachians [17], limits the extent to which traits can be incorporated into macroevolutionary studies [1] and obscures the morphological evolution that led to modern shark biodiversity.

The Upper Cretaceous Chalk of the UK is one of few locations to preserve numerous crown-group selachian cartilaginous skeletons three-dimensionally [18–20], yet their skeletal anatomy has received little attention. The Chalk of the UK represents a shallow, subtropical ocean setting, and has been recognized as a Fossil-Lagerstätte for bony fishes [21]. Although it preserves a number of crown-group selachians [18,20], detailed description of their skeletal morphology has been limited to the problematic taxon *Synechodus* [19,22], a member of the now-extinct Synechodontiformes [23]. As a result, the skeletal anatomy of almost all of the Chalk selachians remains poorly understood compared with detailed descriptive work on flattened Upper Cretaceous elasmobranchs from Lebanon [9,24] and three-dimensional Upper Cretaceous batoids from Moroccan chalk [25,26]. Moreover the three-dimensional imaging methods that have led to an the increasingly sophisticated understanding of extant elasmobranchs skeletal morphology [27–30] and their Palaeozoic forebears [15,31–34] have yet to be deployed on these Chalk taxa. The Chalk provides a unique opportunity to characterize the skeletal anatomy of extinct crown-group selachians and help understand the complex evolutionary history of their living relatives [35].

Although the fishes of the Chalk are preserved three-dimensionally they are difficult to study using conventional means [21]. Here we use computed tomography to describe the skeletal anatomy of two sharks from the Chalk. We use skeletal characters to place these in a selachian phylogeny and show that these belong to a new species of stem-group parascylliid, sister group to other Orectolobiformes. We combine this with a new computed tomographic dataset for living parascylliids to show that these extinct parascylliids preserve plesiomorphic characteristics lost in their extant kin, with implications for the early evolution of galeomorphs.

2. Material and methods

2.1. Institutional abbreviations

CSIRO: CSIRO, Australian National Fish Collection, Hobart, Australia
MNHN: Muséum national d'histoire naturelle, Paris, France
NHMUK: Natural History Museum, London, United Kingdom

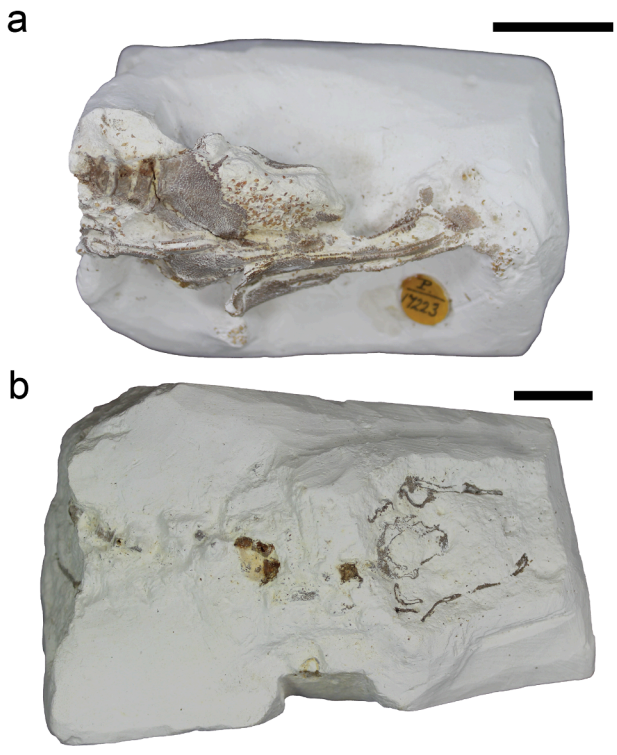

Figure 1. Photographs of the two fossils described in this study. (a) NHM PV P 17223; (b) NHM PV P 73821 a. Photographs taken before removal of isolated teeth from matrix. Scale bars 10 mm.

2.2. Fossil specimens

Two fossil specimens are described here, both held at the Natural History Museum, London (figure 1, electronic supplementary material, figures S1 and S2). At the time of writing NHMUK PV P 17223 is recorded as '*Synechodus*' (figure 1a). It comprises a main block containing most of the fossil (NHMUK PV P 17223), an isolated tooth extracted from the matrix (NHMUK PV P 17223 A), and a dermal denticle extracted from the matrix (NHMUK PV P 17223 B), as well as several fragments broken from the main block which additional scanning shows contain dermal denticles and cartilage fragments. It is listed as being collected from the *Actinocamax quadratus* zone [36] of Britford, near Salisbury, by Dr. H.P. Blackmore. The *Actinocamax quadratus* zone corresponds to the modern *Offaster pilula* and *Gonioteuthis quadrata* zones [37], which in turn correspond to the early Campanian [18]. NHMUK PV P 73821 (figure 1b) is recorded as 'Chondrichthyes', and comprises a main block containing most of the fossil (NHMUK PV P 73821 a), two samples of dermal denticles (NHMUK PV P 73821 b+c), and an isolated tooth extracted from the matrix (NHMUK PV P 73821 D). The only information on its provenance is that it was collected in Newhaven, which would be consistent with a Campanian or Santonian age [38]. This should be confirmed more precisely in future through biostratigraphic correlation of nannofossils [39].

2.3. Extant *Parascyllium*

To aid interpretation of the fossils, we studied the skeleton of an extant parascylliid shark *Parascyllium variolatum* CSIRO CA 3311 (electronic supplementary material, figure S3). CSIRO CA 3311 is a 627 mm TL adult male collected onboard the Fishery Research Vessel *Solea* by demersal trawl on the 3rd December 1981 off southern Australia, 32°58'12.0"S 128°59'47.8"E at 72 m depth.

2.4. Micro-CT (computed tomography) scanning

Fossil specimens were scanned at the Natural History Museum, London, on a Nikon XT H 225 ST CT scanner. NHMUK PV P 17223 was scanned at 210 kV and 524 µA at a voxel size of 29.99 µm. A tungsten rotating reflection target was used with a 1 mm Sn filter, a 250 ms exposure and 3409

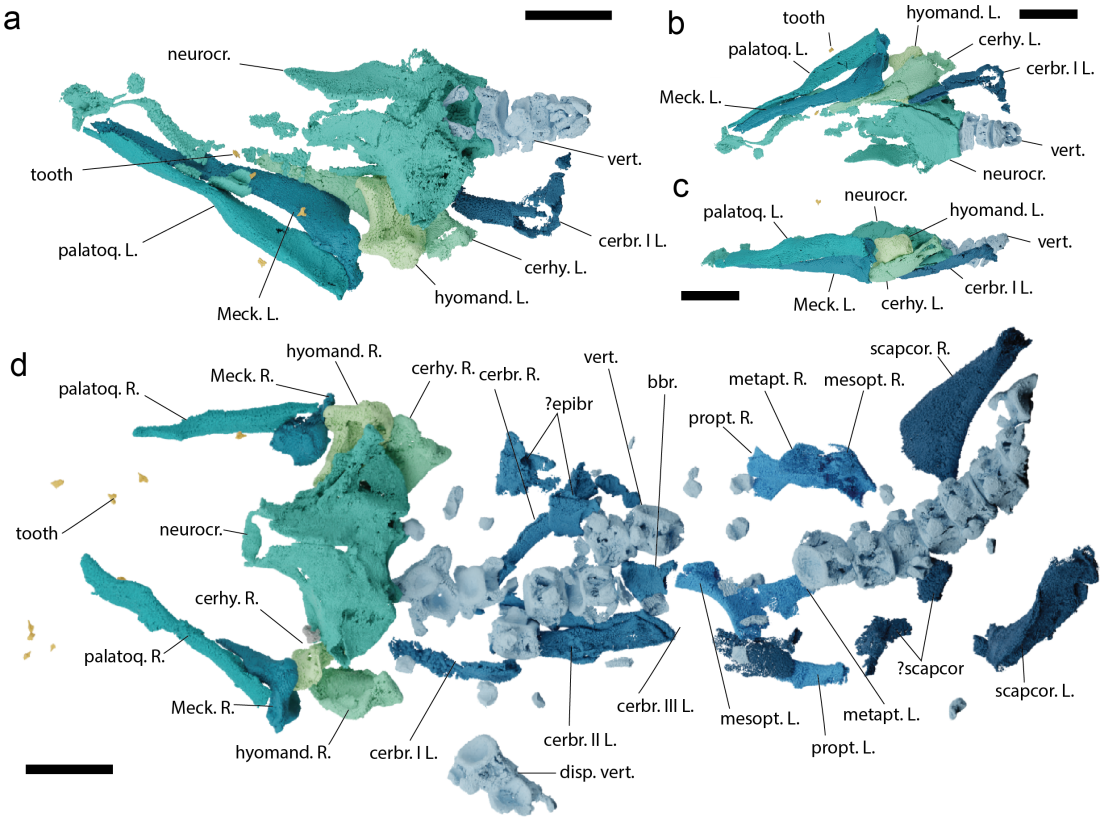

Figure 2. The skeletal anatomy of *Pararhincodon torquis* n. sp. based on computed tomography. (a–c) The head of NHMUK PV P 17223 in dorsal (a), ventral (b), and left lateral (c) views; (d) the head and thorax of NHMUK PV P 73821 a in dorsal view. Abbreviations: bbr., basibranchial; cerbr., ceratobranchial; cerhy., ceratohyal; disp., displaced vertebrae; epibr., epibranchial; hyomand., hyomandibula; L., left; Meck, Meckel's cartilage; mesopt., mesopterygium; metapt., metapterygium; neurocr., neurocranium; scapcor., scapulocoracoid; palatoq, palatoquadrate; propt., propterygium; R., right; vert., vertebrae; I-III, components of branchial arches one to three. All scale bars 5 mm.

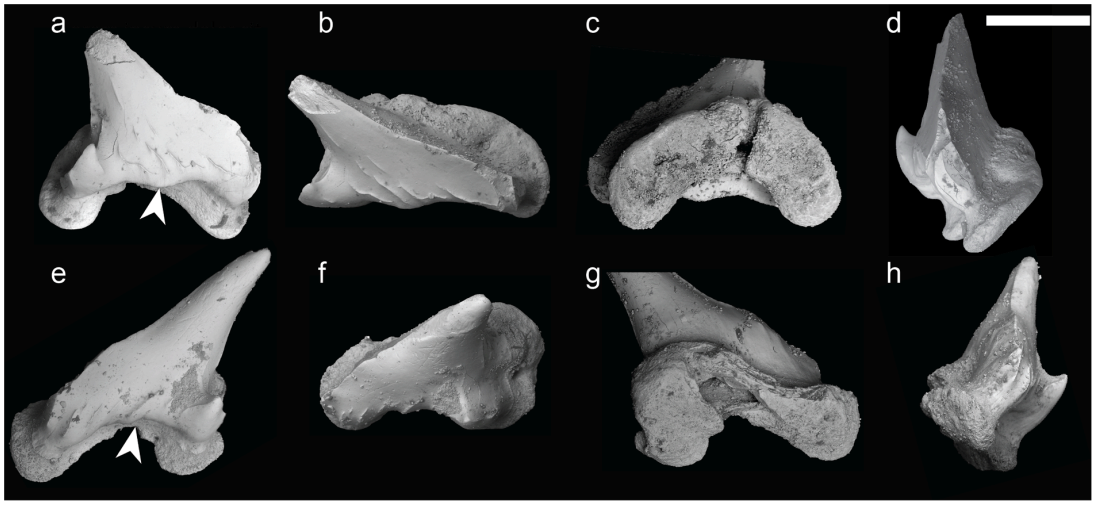

Figure 3. Scanning electron micrographs of the teeth of *Pararhincodon torquis* n. sp. (a–d) Isolated tooth of *P. torquis* n. sp. NHMUK PV P 17223 A in labial (a), occlusal (b), lingual (c), and anterior (d) views; (e–h) isolated tooth of *P. torquis* n. sp. NHMUK PV P 73821 D in labial (e), occlusal (f), lingual (g), and anterior (h) views. Arrow denotes medial protruberance. Scale bar = 0.5 µm.

projections. NHMUK PV P 73821 a was scanned in two sections, each at 155 kV and 129 µA at a voxel size of 31.72 µm. A tungsten reflection target was used with a 0.5 mm Al filter, a 500 ms exposure and 3700 projections. Extant specimen CSIRO CA 3311 was scanned at The University of Queensland, Australia by the Centre for Advanced Imaging on a Yxlon-Comet FF35. Two different

scans were carried out: the first targeted the whole body, with 86 kV, 370 µA, 200 ms exposure time and a 0.5 mm Al filter achieving a voxel size of 85 µm; the second targeted the head and pharynx, with 80 kV, 370 µA, 333 ms exposure time and a 0.5 mm Al filter achieving a voxel size of 25 µm. Scan data were segmented in Materialise Mimics v25.0 (Materialise Software, Leuven, Belgium, https://www.materialise.com/en/healthcare/mimics), using manual thresholding as well as interpolation. All images of three-dimensional data (figure 2) were rendered in Blender v4.2 (blender.org).

2.5. Manual preparation

The specimens were manually prepared at the NHMUK to extract one tooth from each. A combination of mechanical and chemical preparation was used to remove an isolated tooth from within the matrix for each specimen. Preparation was then carried out under a Leica M80 stereo microscope, with a 'cube' of matrix containing the tooth being excavated using a pin vise. The cube was then placed in a small container of 2% acetic acid using calcium orthophosphate as a buffer. The tooth was then bathed in water and cleaned with a fine bristle brush. The two isolated teeth, NHMUK PV P 17223 A and NHMUK PV P 73821 D (figure 3, electronic supplementary material, figures S4 and S5) were then imaged using scanning electron microscopy (SEM) on a JEOL JSM-IT500 scanning electron microscope at the NHMUK.

2.6. Phylogenetic analysis

We assembled a phylogenetic matrix with 19 taxa and 98 morphological characters for galeomorphs with a focus on carpet sharks, primarily from Goto [40] but also using additional sources (see electronic supplementary details for character list). We included representatives of major orectolobiform groups as well as other galeomorphs, and used two squaliforms as an outgroup. Details of taxa and phylogenetic characters are given in the electronic supplementary materials.

We analysed the matrix using maximum parsimony and Bayesian approaches. Maximum parsimony analyses were carried out in Paup* 4.0 [41]; we performed a heuristic search using a TBR algorithm and 100 000 random addition sequence replicates, holding five trees at each step. Bayesian estimates of phylogeny were carried out in MrBayes 3.2.7a [42]. The matrix was analysed using an Mkv model with gamma distributed variable rates and a uniform tree prior. We carried out two separate runs, each for 10 000 000 generations, and checked for convergence initially by checking the standard deviation of split frequency was below 0.01, and then by confirming adequate mixing in Tracer v1.7 [43] both visually and checking all ESS scores were >200. We combined the trees from these runs using tools in R using the package [ape v5.8] [44] and calculated a majority rule consensus tree with a relative burn-in of 0.25.

3. Results

3.1. Systematic palaeontology

Class. **Chondrichthyes** Huxley, 1880
Subclass. **Elasmobranchii** Bonaparte, 1838
Superorder. **Galeomorphii** Compagno, 1973
Order. **Orectolobiformes** Applegate, 1972
Family. **Parascylliidae** Gill, 1862
Genus: ***Pararhincodon*** Herman in Cappetta, 1976

Diagnosis Extended from Cappetta 1980.

Parascylliid with elongate body. Neurocranium with rostral rod, supraorbital crest absent, a mineralized cranial roof with an elongate epiphyseal foramen, a suborbital shelf, pointed postorbital processes and widely spaced endolymphatic ducts with endolymphatic fossa absent. Long, narrow palatoquadrates with no posterior process. Meckel's cartilage lacking posterior process. Vertebrae well-mineralized with primary calcification developed into four diagonal lamellae, notochordal space closed and well-developed intermedialia. Anteriormost cervical vertebra broad with ventrolateral articulatory processes. Pectoral girdle approximately at level of twelfth vertebra, pro-, meso- and metapterygia with strongly curved mesopterygium forming interspace with metapterygium.

Remarks This taxon shares with orectolobiforms an elongate rostral rod and the distinctive basipterygial interspace between the meso- and metapterygium. With parascylliids it shares the widely spaced endolymphatic ducts with no endolymphatic fossa, distinctively pointed postorbital processes, supraorbital crest absent, Meckel's cartilage without posterior process, very small asymmetrical teeth. Unlike extant parascylliids the roof of the braincase and posterior orbital walls are mineralized, it has a separate propterygium in the pectoral fin, and the palatoquadrate lacks a posterior process. As in extant *Parascyllium* (*contra* [40]) and in the asterospondylic vertebrae of extant carcharhiniforms the primary calcification of the vertebral centrae in *Pararhincodon* is developed into x-shaped diagonal lamellae.

Species: ***Pararhincodon torquis*** n. sp.
LSID: rn:lsid:zoobank.org:act:2F23B706-7416-4559-8EE1-8F4D6C77F41
Derivation of name: From torc, a metal collar associated with cultures from the European Iron Age.
Holotype specimen: NHMUK PV P 73821 a

Diagnosis of species Very small, strongly asymmetrical teeth. Cusp triangular with sharp cutting edge, strongly bent lingually and distally. Lateral cusplet on distal edge of tooth, absent on mesial edge which is developed into slight shoulder. Base of cusp has a labial bulge and the medial section is developed into a low labial protuberance. Parallel folds present at the base of the cusp, some of which travel up the cusp's face. Root flat and developed into mesial and distal lobes with deep, open nutrient groove.
Remarks. This new taxon differs from other *Pararhincodon* taxa in that the medial base of the labial crown is expanded into a low protuberance. The cusp is broader than in *P. crochardi*, and the folds resemble *P. ornatus*, although they are not developed into a horizontal crest [18]. Only lateral and posterior teeth are preserved, as asymmetry likely decreased towards the symphysis, a feature that is very pronounced in living parascylliids.

3.2. Description

Both specimens present three-dimensionally preserved cartilages with minor crushing (figure 2, electronic supplementary material, figures S1 and S2). Only calcified parts of the skeleton are preserved, i.e. the mineralized tesserae of the calcified cartilage and the areolar calcification of the vertebrae. All tesserae are single layered but there is variation in thickness, with tesserae on the mandibular arch being notably thicker than those of the neurocranium. The matrix has been bioturbated and numerous isolated dermal denticles (electronic supplementary material, figure S6) are preserved in the matrix and in between the parts of the specimen as well as teeth, and pieces of invertebrates.

The neurocrania in both specimens is partially preserved, with the otic and occipital regions being most complete. The anterior edge of the neurocranial floor is preserved in NHMUK PV P 17223 curving forward to the fragmented rostral rod and base of the internasal septum and below the fragmentary posterolateral wall of the nasal capsule (figures 2 and 4a,e, electronic supplementary material, figures S7 and S8). The orbital wall is more extensively mineralized than in extant parascylliids, with tesselate cartilage surrounding what is likely a separate foramen for the oculomotor nerve (III) as well as foramina for the entry of the superficial ophthalmic+profundus nerve complex and the trigeminal and facial nerve (figure 3, electronic supplementary material, figures S7 and S8). A supraorbital shelf is completely absent, with the orbital wall instead smoothly curving up onto the roof of the neurocranium, which is raised into a longitudinal hump like that in orectolobiforms such as *Chiloscyllium* [30], and split by a long epiphyseal foramen. Unlike living parascylliids the neurocranial roof is calcified anteriorly beyond the level of the trigeminal/facial nerve foramen (figure 4). A section of the left suborbital shelf is preserved in NHMUK PV P 17223, suggesting that it was slightly more laterally extensive than in living parascylliids but the presence or absence of a foramen for the orbital artery or the position of the internal carotids entry into the basicranium are unknown (figure 4a,d). As in *Parascyllium* the otic region features pronounced postorbital processes that taper to a point, and the endolymphatic openings are paired and broadly separated, lying posterolateral relative to the epiphyseal foramen, with no endolymphatic fossa or ascending process (figure 4). Laterally to these the neurocranial roof is raised into low ridges over the anterior and posterior semicircular canals. Even allowing for some crushing, the postorbital region appears to be squatter than in *Parascyllium*

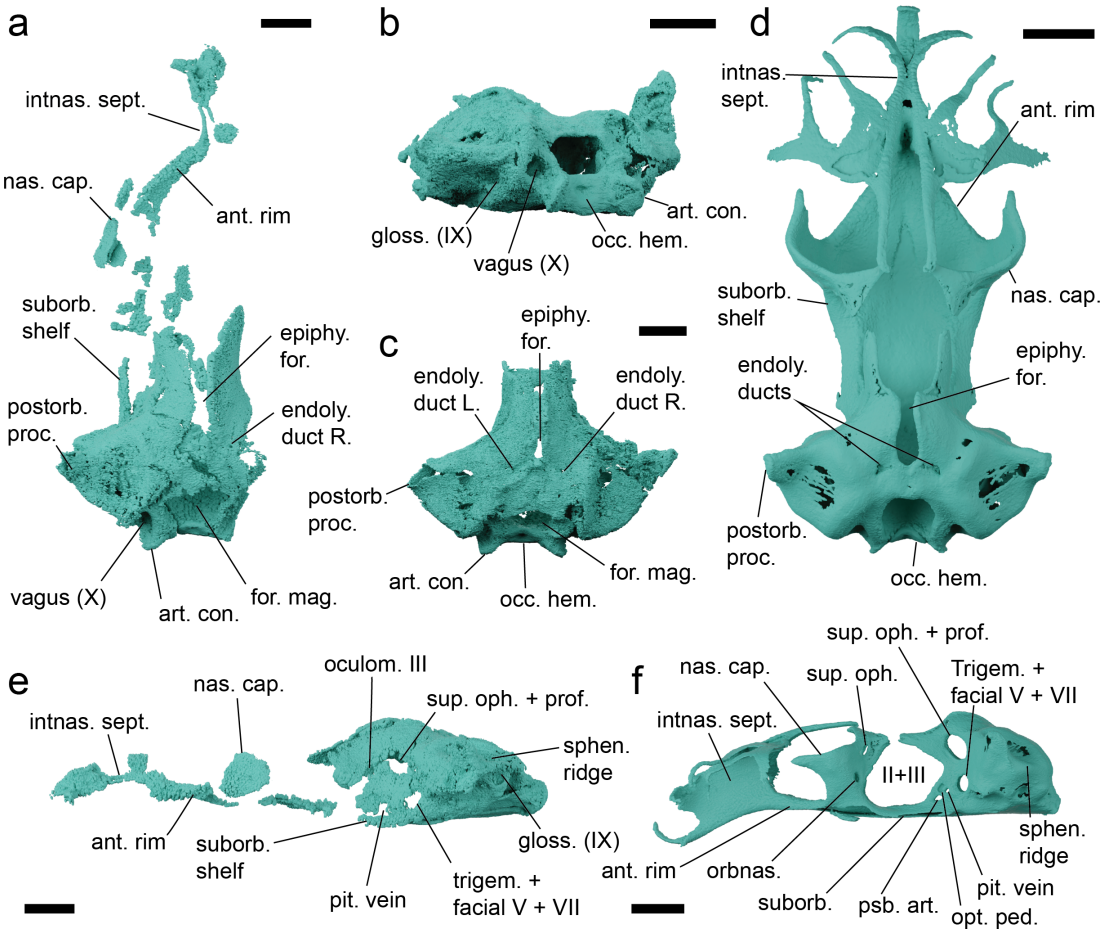

Figure 4. Details of the neurocranial anatomy of *Pararhincodon torquis* n. sp. by comparison with the extant parascylliid *Parascyllium variolatum*. (a) The neurocranium of *P. torquis* n. sp. NHMUK PV P 17223 in dorsal view; (*b*,*c*) the neurocranium of *P. torquis* n. sp. NHMUK PV P 73821 a in postero-lateral (b) and dorsal (c) view; (d) the neurocranium of *P. variolatum CSIRO* CA 3311 in dorsal view; (e) the neurocranium of *P. torquis* n. sp. NHMUK PV P 17223 in left lateral view; (f) the neurocranium of *P. variolatum* CSIRO CA 3311 in left lateral view. Abbreviations: ant. rim, anterior rim of basicranial floor; art. con., articular condyle; endoly., endolymphatic; epi. for., epiphyseal foramen; for. mag., foramen magnum; gloss. (IX), foramen for glossopharyngeal (IX) nerve; II+III, foramen for optic (II) and oculomotor (III) nerves; intnas. sept., internasal septum; nas. cap., nasal capsule; occ. hem., occipital hemicentrum; oculom. III, foramen for oculomotor (III) nerve; opt. ped., optic pedicel; pit., pituitary; postorb. proc., postorbital process; psb. art., foramen for pseudobranchial artery; suborb., suborbital; sphen. ridge, sphenotic ridge; suborbital; sup. oph+prof., foramen for superficial ophthalmic and profundus nerve; trigem.+facial V+VII; foramen for trigeminal and facial nerves; vagus (x), foramen for vagus (x) nerve. All scale bars 5 mm.

with a more pronounced sphenopterotic ridge (figure 4e,f). The hyomandibular facet is positioned immediately posteriorly to the orbit and is overhung by the triangular expansion of the postorbital process and is not set into the basicranial floor to the same extent as seen in *Parascyllium* (figure 4). The postorbital process itself is large and triangular and the lateral surface of the otic capsule below it is slightly embayed. The posterior extent of the postorbital process is defined by the exterior semicircular canal, and below this slants downwards. The small internal foramen by which the glossopharyngeal nerve (IX) enters the cerebral cavity is visible in NHMUK PV P 73821 a, and the nerve exits by its foramen at the posterior base of the postorbital process. The occipital region is broad with the foramen magnum flanked by foramina for the vagus (X) nerve (electronic supplementary material, figure S7h). Ventral to it are broad paired occipital condyles and a median occipital hemicentrum.

The jaws of both specimens are preserved and resemble those of *Parascyllium*. Palatoquadrates are straight with a low profile (figure 5, electronic supplementary material, figure S9) with a dental sulcus, low ethmo-palatine process and a broad ridge along the posterodorsal edge creating the mandibular adductor fossa. The posterior end of the palatoquadrate is blunt and developed into an angle, but lacks the posterior process present in extant parascylliids [40] (electronic supplementary material, figure S9). A concavity in the lingual surface forms the articulation with the Meckel's cartilage. The Meckel's

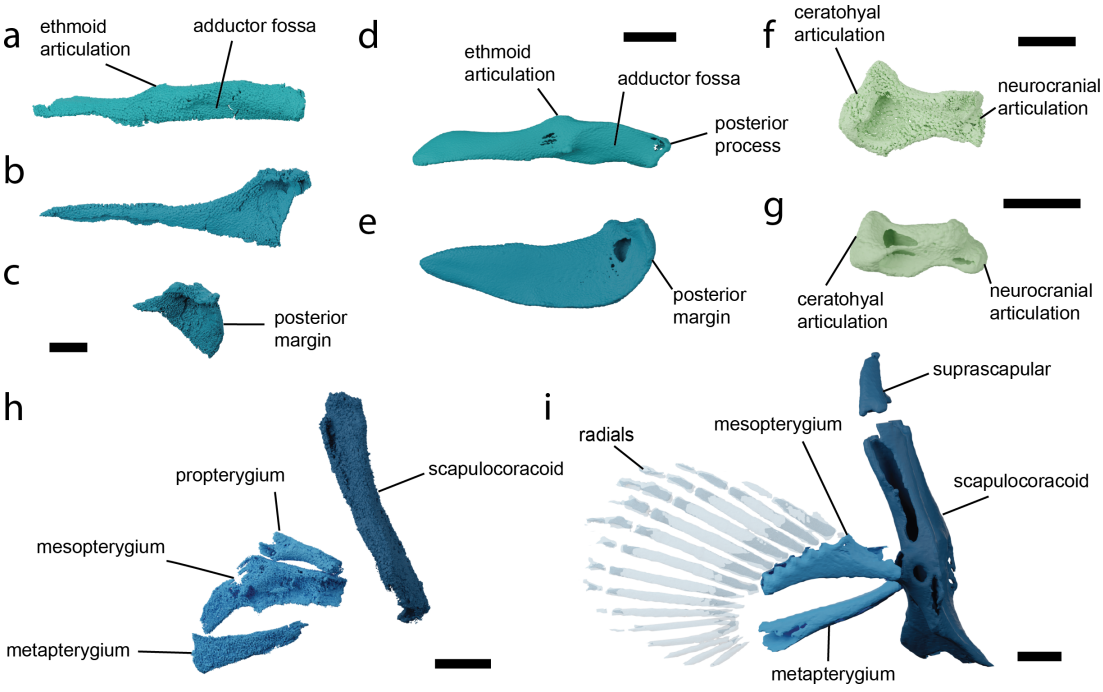

Figure 5. Details of the visceral and pectoral skeleton of *Pararhincodon torquis* n. sp. by comparison to the extant parascylliid *Parascyllium variolatum*. (a) The left palatoquadrate of *P. torquis* n. sp. NHMUK PV P 17223 in labial view; (b) the Meckel's cartilage of *P. torquis* n. sp. NHMUK PV P 17223 in labial view; (c) the articular region of Meckel's cartilage of *P. torquis* n. sp. NHMUK PV P 73821 a in labial view; (d) the palatoquadrate of *P. variolatum CSIRO* CA 3311 in labial view; (e) the Meckel's cartilage of *P. variolatum* CSIRO CA 3311 in labial view; (f) the left hyomandibula of *P. torquis* n. sp. NHMUK PV P 17223 in dorsal view; (g) the left hyomandibula of *P. variolatum CSIRO* CA 3311 in dorsal view; (h) right pectoral fin skeleton of *P. torquis* n. sp. NHMUK PV P 73821a arranged into approximately life position in right lateral view; (i) right pectoral fin skeleton of *P. variolatum* CSIRO CA 3311 in right lateral view. All scale bars 5 mm.

cartilage is straight (figure 5, electronic supplementary material, figure S10) with a pronounced mandibular knob and a broad lateral flange carrying the articular cotylus. The posterior margin of both Meckel's cartilages is preserved in NHMUK PV P 73821a and shows it did not bear a posterior process (figure 5c,e). No labial cartilages are preserved in either specimen.

Although no teeth are preserved in articulation with the mandibular cartilages in either specimen, we interpret teeth in both specimens as originating from the articulated specimens due to their consistent morphology and size and their location close to the mandibular cartilages (figure 3, electronic supplementary material, figures S4 and S5). In NHMUK PV P 73821 a, we identify nine teeth in the matrix and in NHMUK PV P 17223 four teeth (electronic supplementary material, figure S5). Teeth are very small, being approximately 1 mm in height (figure 3, electronic supplementary material, figure S4). All preserved teeth are strongly asymmetrical and represent lateral or posterior teeth [45,46], which is consistent with both specimens missing the front part of the jaws. A detailed description of tooth morphology is given in the diagnosis.

The full length of the pharynx is preserved in NHMUK PV P 73821 a, and parts of the hyoid skeleton are preserved in both specimens. The hyomandibula is short and robust, with the distal surface expanded for its articulation with the palatoquadrate/ceratohyal to a greater extent than in extant *Parascyllium* (figures 2 and 5, electronic supplementary material, figure S11). The ceratohyal is arched and broad, with a low groove on the labial surface (figure 2, electronic supplementary material, figure S12). The basihyal is missing in both specimens. The branchial skeleton is preserved in both specimens but more extensively in NHMUK PV P 73821 a (figure 2, electronic supplementary material, figure S13). In NHMUK PV P 17223 the anteriormost left branchial arch is preserved, including most of ceratobranchial I, epibranchial I and the proximal tip of pharyngobranchial I. In NHMUK PV P 73821 a the branchial skeleton is heavily disrupted but on the left side three epibranchials (likely I–III) are preserved, while on the right side there are several branchial cartilages including identifiable cerato-, epi- and pharyngobranchials. Also preserved is the tip of the anterior process of the basibranchial copula. The branchial cartilage proportions and morphology match those of *Parascyllium* (figure 2, electronic supplementary material, figure S13).

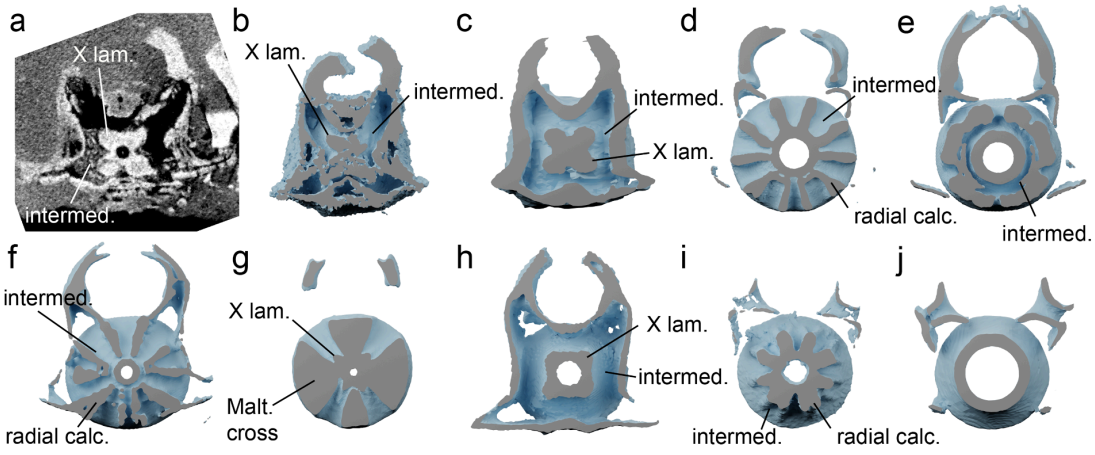

Figure 6. Bisected vertebrae of *Pararhincodon torquis* n. sp. by comparison to extant sharks, showing mineralized regions based segmented from CT data. All vertebrae taken from the level of approximately the heart. (*a,b*) *P. torquis* n. sp. NHMUK PV P 73821 a as a CT section (a) and bisected three-dimensional volume (b); (c) *Parascyllium variolatum CSIRO* CA 3311; (d) orectolobiform *Chiloscyllium plagiosum*; (e) orectolobiform *Sutorectus tentaculatus;* (f) orectolobiform *Brachaelurus waddi*; (g) carcharhiniform *Prionace glauca*; (h) carcharhiniform *Proscyllium magnificum*; (i) heterodontid *Heterodontus francisci*; (j) squaliform *Squalus cubensis*. Abbreviations: intermed., intermedialia; Malt. cross, Maltese-cross-shaped secondary calcification; rad. calc., radial secondary calcification; X lam, X-shaped laminae. Not to scale. See electronic supplementary material, table S1 for specimen details. Not shown to scale.

The pectoral skeleton is preserved only in NHMUK PV P 73821 a (figure 2d, electronic supplementary material, figure S14). Flattening of the shoulder girdle during preservation has resulted in the dorsal processes of the scapulocoracoids being pushed posteriorly relative to the fin skeleton and shattered pieces of cartilage are likely corresponding to parts of the articular regions and the coracoid bar. The basipterygia of both left and right pectoral fins are preserved. Meso- and metapterygia are identifiable by comparison with those of *Parascyllium*, although they have slightly different proportions. Associated with these are additional elements: based on their morphology we are able to eliminate the possibility that they are posterior branchial elements, and based on their location they are unlikely to be superscapulae. We conclude that these are propterygia, which are absent in extant parascylliids [40]. No fin radials are preserved.

Sections of the vertebral column are preserved in both specimens: NHMUK PV P 17223 preserves the anteriormost three vertebral centra while NHMUK PV P 73821 a preserves a largely articulated section of the vertebral column extending to the level of the pectoral girdle, comprising 18 vertebral centra (figures 2 and 6, electronic supplementary material, figure S15). Interdorsal and basidorsal elements are also present but mostly scattered through the matrix (electronic supplementary material, figure S2). Vertebrae comprise cone-shaped zones of primary calcification, with the notochordal space either absent or very small. The outer surfaces of the vertebrae are well mineralized. The anteriormost vertebral centrum has expanded processes for articulation with the occipital condyles.Cross-sections of the vertebrae of *Pararhincodon* from throughout the preserved column show that the primary calcification extends via four short mineralized lamellae, arranged into an x-shape, into the intermedialia (figure 6a,b). Although this fits within the range of conditions described as 'asterospondylic' [45], the numerous secondary calcifications that extend radially into the intermedialia in most orectolobiforms, either to the level of the *membrana elastica externa* (hemiscylliids, *Stegostoma*, *Ginglymostoma*, figure 6c) or not reaching this level (orectoloboids and *Brachaelurus*), are absent (figure 6d–f). Goto [40] described the vertebrae of living parascylliids as lacking any kind of extension from the primary calcification, however our CT data shows that secondary calcifications resembling those of *Pararhincodon* are in fact present throughout the vertebral column of *Parascyllium* (figure 6c). Similar x-shaped laminae extending from the primary calcification are also present in Carcharhiniformes [45,47,48], although the vertebrae of the parascylliids we describe lack the Maltese-cross shaped calcified areas in taxa like *Prionace* (figure 6e), instead more closely resembling the vertebrae of *Proscyllium* (figure 6f).

3.3. Phylogenetic analysis

The parsimony analysis recovered eight most parsimonious trees, with a length of 192. Both Bayesian and parsimony approaches recovered tree topologies broadly consistent with estimates of selachian

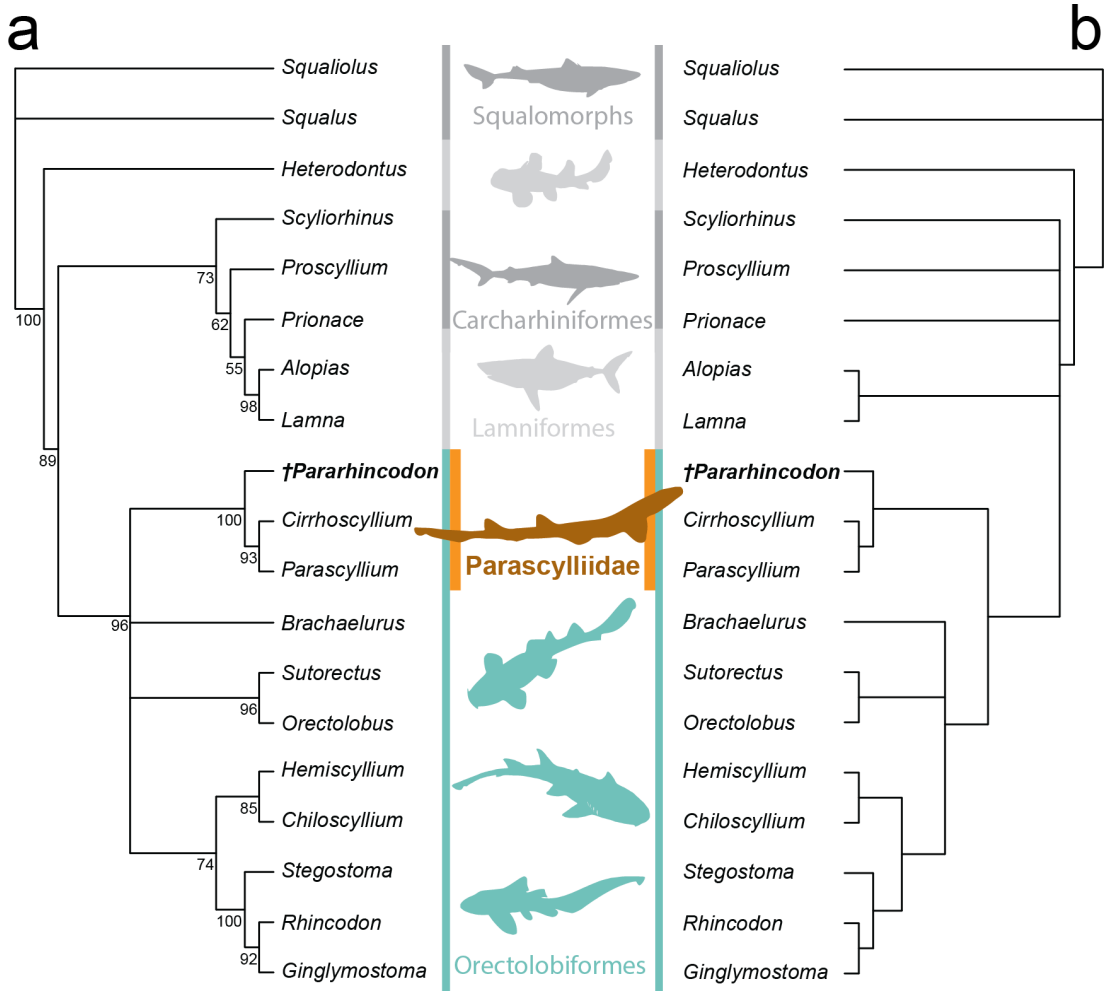

Figure 7. Results of phylogenetic analysis of morphological phylogenetic dataset. (a) 50% Majority rule consensus tree from Bayesian analysis with node values representing posterior probability of that clade; (b) strict consensus of eight most parsimonious trees recovered by parsimony analysis. Silhouettes from Phylopic: see electronic supplementary material, table S2 for attributions.

phylogeny based on molecular data [1,49]. Galeomorphs were found to be monophyletic, with *Heterodontus* as the sister group to all other galeomorphs. Within galeomorphs, orectolobiforms are found to be the sister group to carcharhiniforms plus lamniforms. Our dataset recovered carcharhiniforms as being paraphyletic relative to lamniforms, likely as a result of poor taxon sampling.

Both analytical approaches recover orectolobiforms as a clade, with extant parascylliids, and hemiscylliids, *Stegostoma*, *Rhincodon* and *Ginglymostoma* as sub-clades, reflecting molecular-based understanding of the group's intrarelationships. *Brachaelurus* and wobbegongs (*Sutorectus* and *Orectolobus*) are recovered in a polytomy with these clades: although unresolved this is consistent with molecular trees which suggest they form a clade that is the sister group to all other orectolobiforms except parascylliids [1,49]. Both approaches found *Pararhincodon torquis* n. sp. to be a stem-group parascylliid within orectolobiforms, i.e. the sister group to a clade formed by *Parascyllium* and *Cirrhoscyllium*, with a high degree of confidence (figure 7).

4. Discussion

4.1. *Pararhinchodon* and the Parascylliidae

Based on our analysis we are able to confidently identify *Pararhincodon torquis* n. sp. as a stem-group parascylliid (figure 7). Previously, articulated *Pararhincodon* were known only from Lebanon [24], and to date only one species, *Pararhincodon lehmani* from the Cenomanian of Haqel, was formally described based on articulated remains [50]. This description was based on a single poorly preserved specimen,

MNHN HAK 556, which was attributed to Orectolobiformes on the basis of the presence of a rostral rod on the neurocranium, and then to the Parascylliidae on the basis of teeth lacking a labial apron [50]. As a result, *Pararhincodon*'s status as a parascylliid has been treated cautiously [24] and the taxon has been omitted from attempts to reconstruct orectolobiform evolutionary history [35]. In addition to *Pararhincodon lehmani* and *P. torquis* n. sp., three species based on isolated teeth are known ranging from the Cenomanian to the Lutetian—*P. crochardi*, *P. germaini* and *P. ypresiensis* [46,51–53] and the oldest teeth assigned to *Pararhincodon* sp. are Albian [54]. Our robust identification of *Pararhincodon* as a parascylliid using skeletal morphology allows this tooth record to be associated with the parascylliid stem-group with confidence.

Extant parascyllliids comprise two genera, *Parascyllium* and *Cirrhoscyllium*, which molecular and morphological data indicate are the sister-groups to all other orectolobiforms [1,35,40]. These taxa are distinguished from other orectolobiforms by numerous distinctive skeletal anatomies of the neurocranium, visceral skeleton and pectoral girdle [40], and have a markedly anguilliform body shape which within orectolobiforms is comparable only with some hemiscylliids [55]. Our new data show that much of this skeletal anatomy, for example the distinctive morphology of the otic region of the neurocranium and the internal mineralization of the vertebrae [40], were already in place well before the divergence of the crown-group. However, other aspects, such as the loss of the propterygium in the pectoral fin and demineralization of the neurocranium, were more recently acquired and may be features of the parascylliid crown-group. Comparison with the body profile of undescribed *Pararhincodon* specimens from Haqel and Hjoula [24, pl. 20] suggests that the body of *Pararhincodon* was less anguilliform with more anteriorly placed dorsal fins than extant parascylliids. Contemporaneous Lebanese parascylliids show that the more pronouncedly anguilliform body shapes in parascylliids had already evolved by this point and these may represent closer relatives of the parascylliid crown-group [24]. These new data provide an insight into the mosaic evolution of modern parascyllids' distinctive anatomies.

The divergence of *Parascyllium* and *Cirrhoscyllium* is comparatively recent, placed by molecular estimates in the Late Cretaceous or Palaeogene [1,35], with the oldest tooth assigned to a living genus (*Parascyllium*) from the Lutetian (Eocene) of France [46,51]. Their divergence from other orectolobiforms is much older than this date or the range of *Pararhincodon,* with molecular estimates placing it in the Triassic [1,35]. Spanning this gap by confidently assigning Jurassic taxa to the parascylliid stem-group is challenging due to the small size and fairly unremarkable anatomy of parascylliid teeth, illustrated by the initial assignment of *Pararhincodon* to the Scyliorhinidae [52]. In most *Pararhincodon* species a labial apron is absent, however the labial protuberance on the teeth of *Pararhincodon torquis* n. sp. bears comparison with the distinctive apron of orectolobiform teeth and suggests that this could be a plesiomorphic feature of their dentitions rather than a feature uniting other Orectolobiformes to the exclusion of parascylliids. If so, candidate stem-group parascylliids could include taxa with labial aprons, for example *Phorcynis*, which has a larger labial protuberance than *Pararhincodon torquis* n. sp. but a similarly asymmetrical shape of the crown [46]. Other Mesozoic tooth taxa have crown morphologies that depart further from that of *Pararhincodon* but possess labial protuberances and slender cusps, for example *Akaimia* [56,57].

4.2. Orectolobiformes and galeomorphs

Because the divergence of parascylliids from other orectolobiforms is equivalent to the divergence of the orectolobiform crown-group the timescale of their evolution has important implications for the evolution of the galeomorph crown-group. Various holomorphic Upper Jurassic fossils have been identified as Orectolobiformes including *Phorcynis*, *Palaeorectolobus* and possibly *Palaeoscyllium* [12,58] while the oldest isolated teeth assigned to Orectolobiformes are Toarcian examples of *Annea* and *Folipistrix* [46,59–61]. However, a lack of phylogenetically informative characters means that these Jurassic taxa, whether teeth or holomorphic specimens, cannot at present be assigned to specific internal branches of the orectolobiform tree. Recent molecular estimates place major crown-group orectolobiform divergence events, i.e. the split between the clade including Brachaeluridae and Orectolobidae and the clade including Hemiscylliidae, Ginglymostomatidae and Rhincodontidae (figure 7), as well as early divergences within those clades, in the Jurassic/Lower Cretaceous. Jurassic Orectolobiformes could feasibly represent stem-group members of those lineages, but could also feasibly represent stem-group Orectolobiformes. Although it is considerably younger than these taxa, strictly speaking the Campanian *Pararhincodon torquis* n. sp. is a candidate for a robust minimum constraint for the orectolobiform crown-group because it can be confidently assigned to a specific

branch of the crown-group [62]. Less conservatively the articulated Cenomanian putative ginglymostomatid *Cantioscyllium decipiens* could also provide a hard minimum constraint for the orectolobiform crown-group [20], and *Cantioscyllium* teeth have been used to constrain this node in recent time-calibrated phylogenetic analysis [1].

The similarities in vertebral anatomy that we identify between parascylliids and carcharhiniforms fit into an emerging understanding of elasmobranch macroevolution. Galeomorphs' long evolutionary history probably extends back to the Permian, and extant galeomorph groups are thought to have evolved in coastal habitats from relatively small, benthic forms [1–3]. The presence of four diagonal lamellae themselves probably form the basis for more complex asterospondylic vertebral conditions across elasmobranchs during development [47]. However, the adult parascylliid-like configuration differs from all other orectolobiforms including asterospondylic forms [40] and instead is strikingly similar to that of several catshark-like carcharhiniform taxa including *Proscyllium* and *Schroederichthys* [47,48]. No Lamniformes display these x-shaped laminae, instead having vertebrae with numerous radial lamellae [47,63]. Thus, this x-shaped configuration could plausibly represent a plesiomorphic anatomy for galeomorphs excluding Heterodontiformes, retained in certain crown-group members but lost in disparate members of the group. Its retention in adult parascylliids and catshark-like carcharhiniforms may reflect the lower mechanical demands of small body size and benthic lifestyles, with larger galeomorphs supporting larger body and life in the water column by increasing the level of secondary calcification within the intermedialia. This might also explain this state's absence in lamniforms; while some early lamniform teeth are found in nearshore environments all living lamniforms are large and free-swimming [3,64,65].

Finally, these new data show the potential of shark skeletons preserved in the Chalk as a window into the evolution of modern elasmobranch biodiversity. Modern orectolobiform biodiversity is centred in the Indo-Pacific biodiversity hotspot, and most species-level orectolobiform biodiversity originated in this region during the Cenozoic [35,66]. The two extant parascylliid genera are highly geographically restricted within this region, with *Parascyllium* endemic to Australia and *Cirrhoscyllium* to Vietnam, Taiwan and Japan [67,68]. However, the fossil record indicates that this biodiversity centre shifted from the shallow seas of the Atlantic in the Upper Cretaceous to its present location via the Tethys Sea through the Cenozoic, in the wider context of a global shift in marine biodiversity [35,69]. As our description of *Pararhincodon torquis* n. sp. shows, the Chalk has the potential to provide a uniquely detailed glimpse into elasmobranch faunas at the beginning of this process, and to complement and be complemented in turn by the detailed picture provided by the tooth record [18]. Further descriptions of crown-group elasmobranchs from the Chalk should allow the incorporation of several taxa confidently into elasmobranch phylogeny, and estimates of their evolutionary timing.

5. Conclusions

Three-dimensional fossil remains of crown-group elasmobranch skeletons are much rarer than their teeth but are far more information-rich. As it does for actinopterygians [21,70] the Cretaceous Chalk provides a uniquely detailed insight into these skeletal anatomies, allowing the reconciliation of the records of isolated teeth and skeletal morphologies which are poorly understood even in those elasmobranchs known from exquisitely preserved holomorphic fossils [12,24]. Here, the skeletal anatomy of the Cenomanian *Pararhincodon torquis* n. sp. allows the confident identification of *Pararhincodon* as a stem-group parascylliid and provides a rare insight into the morphological transformations that led to modern orectolobiform biodiversity. The Chalk offers a unique opportunity to harvest skeletal information from extinct elasmobranchs which should ultimately feed morphological information into elasmobranch phylogeny, estimates of the timing of their evolution, and efforts to understand phenomena like their slow evolutionary rate [71].

Ethics. Fossils specimens are held in the collections of the Natural History Museum, London, and were collected in the UK. Extant specimens are held in the collections of CSIRO national fish collection, Australia, and were collected in Australia.

Data accessibility. 3D models and files related to the phylogenetic analysis are made publicly available via Dryad [72]. 3D models are provided as plys, and as .blend files which can be opened in the freeware Blender. Phylogenetic analysis files include the phylogenetic matrix as a Nexus (.nex) file, parsimony trees (.tre), and the parameter and tree output files from MrBayes.).

CT datasets are made available on Morphosource, which can be accessed at the Morphosource links below.

Pararhincodon torquis n. sp. NHMUK PV P 17223

https://doi.org/10.17602/M2/M677323
Pararhincodon torquis n. sp. NHM PV P 73821a
Front half: https://doi.org/10.17602/M2/M678241
Rear half:https://doi.org/10.17602/M2/M678245
Parascyllium variolatum n. sp. CSIRO CA 3311
Body https://doi.org/10.17602/M2/M678404
Head: https://doi.org/10.17602/M2/M678704
Supplementary material is available online [73].

Declaration of AI use. we have not used AI-assisted technologies in creating this article.

Authors' contributions. R.P.D.: conceptualization, data curation, formal analysis, funding acquisition, investigation, methodology, visualization, writing—original draft, writing—review and editing; Z.J.: funding acquisition, investigation, methodology, writing—review and editing; H.L.O'N.: investigation, methodology, writing—review and editing; K.M.: investigation, methodology, writing—review and editing; E.L.B.: investigation, resources, writing—review and editing; B.C.: investigation, methodology; C.U.: methodology; M.R.: funding acquisition, project administration, writing—review and editing.

All authors gave final approval for publication and agreed to be held accountable for the work performed therein.

Conflict of interest declaration. We declare we have no competing interests.

Acknowledgements. Thanks to the NHMUK Imaging and Analysis Centre for scanning, particularly Dr. Alex Ball (NHMUK, London) for assistance with SEM and Vincent Fernandez and Agnese Lanzetti for assistance with micro-CT scanning fossils at NHMUK. The authors acknowledge the facilities and scientific and technical assistance of the National Imaging Facility, a National Collaborative Research Infrastructure Strategy (NCRIS) capability, and Dr. Ekaterina Strounina at the Centre for Advanced Imaging, University of Queensland for scanning the Parascyllium variolatum specimen. Thanks also to Guillaume Guinot, Sebastian Stumpf and Eduardo Villalobos-Segura for helpful discussion. Many thanks also to Dr. Brian Gasson who donated NHMUK PV P 73821 to the NHMUK collection. Finally, we would like to thank Jürgen Kriwet and one additional anonymous reviewer who provided helpful comments on the manuscript.

References

1. Marion AFP, Condamine FL, Guinot G. 2024 Sequential trait evolution did not drive deep-time diversification in sharks. *Evolution* **78**, 1405–1425. (doi:10.1093/evolut/qpae070)
2. Sorenson L, Santini F, Alfaro ME. 2014 The effect of habitat on modern shark diversification. *J. Evol. Biol*. **27**, 1536–1548. (doi:10.1111/jeb.12405)
3. Sternes PC, Schmitz L, Higham TE. 2024 The rise of pelagic sharks and adaptive evolution of pectoral fin morphology during the Cretaceous. *Curr. Biol*. 1–9. **34**, 2764–2772.(doi:10.1016/j.cub.2024.05.016)
4. Stein RW, Mull CG, Kuhn TS, Aschliman NC, Davidson LNK, Joy JB, Smith GJ, Dulvy NK, Mooers AO. 2018 Global priorities for conserving the evolutionary history of sharks, rays and chimaeras. *Nat. Ecol. Evol*. **2**, 288–298. (doi:10.1038/s41559-017-0448-4)
5. López-Romero FA, Stumpf S, Kamminga P, Böhmer C, Pradel A, Brazeau MD, Kriwet J. 2023 Shark mandible evolution reveals patterns of trophic and habitat-mediated diversification. *Commun. Biol*. **6**, 496. (doi:10.1038/s42003-023-04882-3)
6. Dedman S *et al*. 2024 Ecological roles and importance of sharks in the Anthropocene Ocean. *Science* **385**, adl2362. (doi:10.1126/science.adl2362)
7. Underwood CJ. 2006 Diversification of the Neoselachii (Chondrichthyes) during the Jurassic and Cretaceous. *Paleobiology* **32**, 215–235. (doi:10.1666/04069.1)
8. Brée B, Condamine FL, Guinot G. 2022 Combining palaeontological and neontological data shows a delayed diversification burst of carcharhiniform sharks likely mediated by environmental change. *Sci. Rep.* **12**, 21906. (doi:10.1038/s41598-022-26010-7)
9. George H, Bazzi M, El Hossny T, Ashraf N, Abi Saad P, Clements T. 2024 The famous fish beds of Lebanon: the Upper Cretaceous Lagerstätten of Haqel, Hjoula, Nammoura and Sahel Aalma. *J. Geol. Soc. London* **181**. (doi:10.1144/jgs2023-210)
10. Shimada K. 1997 Skeletal anatomy of the Late Cretaceous lamniform shark, *Cretoxyrhina mantelli* from the Niobrara Chalk in Kansas. *J. Vertebr. Paleontol*. **17**, 642–652. (doi:10.1080/02724634.1997.10011014)
11. Shimada K, Cicimurri DJ. 2005 Skeletal anatomy of the Late Cretaceous shark, *Squalicorax* (Neoselachii: Anacoracidae). *Paläontol. Z*. **79**, 241–261. (doi:10.1007/bf02990187)
12. Villalobos-Segura E, Stumpf S, Türtscher J, Jambura PL, Begat A, López-Romero FA, Fischer J, Kriwet J. 2023 A synoptic review of the cartilaginous fishes (Chondrichthyes: Holocephali, Elasmobranchii) from the Upper Jurassic konservat-lagerstätten of southern germany: taxonomy, diversity, and faunal relationships. *Diversity* **15**, 386. (doi:10.3390/d15030386)
13. Vullo R *et al*. 2024 Exceptionally preserved shark fossils from Mexico elucidate the long-standing enigma of the Cretaceous elasmobranch *Ptychodus*. *Proc. R. Soc. B* **291**, 20240262. (doi:10.1098/rspb.2024.0262)
14. Coates MI, Gess RW, Finarelli JA, Criswell KE, Tietjen K. 2017 A symmoriiform chondrichthyan braincase and the origin of chimaeroid fishes. *Nature* **541**, 208–211. (doi:10.1038/nature20806)

15. Dearden RP, Herrel A, Pradel A. 2024 The pharynx of the iconic stem-group chondrichthyan *Acanthodes* Agassiz, 1833 revisited with micro-computed tomography. *Zool. J. Linn. Soc*.1–19 (doi:10.1093/zoolinnean/zlae058)
16. Pradel A, Maisey JG, Tafforeau P, Mapes RH, Mallatt J. 2014 A Palaeozoic shark with osteichthyan-like branchial arches. *Nature* **509**, 608–611. (doi:10.1038/nature13195)
17. Villalobos-Segura E, Marramà G, Carnevale G, Claeson KM, Underwood CJ, Naylor GJP, Kriwet J. 2022 The phylogeny of rays and skates (Chondrichthyes: Elasmobranchii) based on morphological characters revisited. *Diversity* **14**, 456. (doi:10.3390/d14060456)
18. Guinot G, Underwood CJ, Cappetta H, Ward DJ. 2013 Sharks (Elasmobranchii: Euselachii) from the Late Cretaceous of France and the UK. *J. Syst. Palaeontol*. **11**, 589–671. (doi:10.1080/14772019.2013.767286)
19. Maisey JG. 1985 Cranial morphology of the fossil elasmobranch *Synechodus dubrisiensis*. *Am. Mus. Novit*. **2804**, 1–28. http://hdl.handle.net/2246/5280
20. Woodward AS. 1911 The fossil fishes of the English Chalk. Part VI. Plates XXXIX–XLVI. *Palaeontogr. Soc. Monogr.* **64**, 185–224. (doi:10.1080/02693445.1911.12035551)
21. Friedman M, Beckett HT, Close RA, Johanson Z. 2015 The English Chalk and London Clay: two remarkable british bony fish lagerstätten. In Arthur smith woodward: his life and influence on modern vertebrate palaeontology (eds Z Johanson, PM Barrett, M Richter, M Smith), vol. 430. London: The Geological Society of London.(Special Publications).
22. Maisey JG. 2008 The postorbital palatoquadrate articulation in elasmobranchs. *J. Morphol*. **269**, 1022–1040. (doi:10.1002/jmor.10642)
23. Klug S. 2010 Monophyly, phylogeny and systematic position of the †Synechodontiformes (Chondrichthyes, Neoselachii). *Zool. Scr*. **39**, 37–49. (doi:10.1111/j.1463-6409.2009.00399.x)
24. Pfeil FH. 2021 The new family Mesiteiidae (Chondrichthyes, Orectolobiformes), based on *Mesiteia emiliae* Kramberger, 1884. A contribution to the Upper Cretaceous (early Cenomanian) shark fauna from Lebanon. In *Ancient fishes and their living relatives: a tribute to John G. Maisey* (eds A Pradel, JSS Denton, P Janvier), pp. 101–182. München, Germany: Verlag Dr. Friedrich Pfeil.
25. Claeson KM, Underwood CJ, Ward DJ. 2013 *Tingitanius tenuimandibulus,* a new platyrhinid batoid from the Turonian (Cretaceous) of Morocco and the cretaceous radiation of the Platyrhinidae. *J. Vertebr. Paleontol*. **33**, 1019–1036. (doi:10.1080/02724634.2013.767266)
26. Villalobos-Segura E, Underwood CJ, Ward DJ, Claeson KM. 2019 The first three-dimensional fossils of Cretaceous sclerorhynchid sawfish: *Asflapristis cristadentis* gen. et sp. nov., and implications for the phylogenetic relations of the Sclerorhynchoidei (Chondrichthyes). *J. Syst. Palaeontol.* **17**, 1847–1870. (doi:10.1080/14772019.2019.1578832)
27. Dearden RP, Mansuit R, Cuckovic A, Herrel A, Didier D, Tafforeau P, Pradel A. 2021 The morphology and evolution of chondrichthyan cranial muscles: a digital dissection of the elephantfish *Callorhinchus milii* and the catshark *Scyliorhinus canicula*. *J. Anat*. **238**, 1082–1105. (doi:10.1111/joa.13362)
28. Denton JSS, Maisey JG, Grace M, Pradel A, Doosey MH, Bart HL Jr, Naylor GJP. 2018 Cranial morphology in *Mollisquama* sp. (Squaliformes; Dalatiidae) and patterns of cranial evolution in dalatiid sharks. *J. Anat*. **233**, 15–32. (doi:10.1111/joa.12823)
29. Maisey JG. 2004 Morphology of the braincase in the broadnose sevengill shark *Notorynchus* (Elasmobranchii, Hexanchiformes), based on CT scanning. *Am. Mus. Novit*. **3429**, 3429. (doi:10.1206/0003-0082(2004)4292.0.co;2)
30. Staggl MA, Abed-Navandi D, Kriwet J. 2022 Cranial morphology of the orectolobiform shark, *Chiloscyllium punctatum* Müller & Henle, 1838. *Vertebr. Zool*. **72**, 311–370. (doi:10.3897/vz.72.e84732)
31. Coates MI, Finarelli JA, Sansom IJ, Andreev PS, Criswell KE, Tietjen K, Rivers ML, La Riviere PJ. 2018 An early chondrichthyan and the evolutionary assembly of a shark body plan. *Proc. R. Soc. B* **285**, 20172418. (doi:10.1098/rspb.2017.2418)
32. Coates MI, Tietjen K, Olsen AM, Finarelli JA. 2019 High-performance suction feeding in an early elasmobranch. *Sci. Adv*. **5**, eaax2742. (doi:10.1126/sciadv.aax2742)
33. Frey L, Coates M, Ginter M, Hairapetian V, Rücklin M, Jerjen I, Klug C. 2019 The early elasmobranch *Phoebodus*: phylogenetic relationships, ecomorphology and a new time-scale for shark evolution. *Proc. R. Soc. B* **286**, 20191336. (doi:10.1098/rspb.2019.1336)
34. Maisey JG. 2011 The braincase of the middle Triassic shark *Acronemus tuberculatus* (Bassani, 1886). *Palaeontology* **54**, 417–428. (doi:10.1111/j.1475-4983.2011.01035.x)
35. Boyd BM, Seitz JC. 2021 Global shifts in species richness have shaped carpet shark evolution. *BMC Ecol. Evol*. **21**, 192. (doi:10.1186/s12862-021-01922-6)
36. Jukes-Browne AJ, Hill W. 1904 The Cretaceous rocks of Britain. Vol. 3 - The Upper Chalk of England. In *Memoir of the geological survey of the United Kingdom*. UK, London.
37. Mortimore RN. 1986 Stratigraphy of the Upper Cretaceous white chalk of Sussex. *Proc. Geol. Assoc*. **97**, 97–139. (doi:10.1016/s0016-7878(86)80065-7)
38. Mortimore R. 2011 A chalk revolution: what have we done to the Chalk of England? *Proc. Geol. Assoc*. **122**, 232–297. (doi:10.1016/j.pgeola.2010.09.001)
39. Bramlette MN, Riedel WR. 1954 Stratigraphic value of discoasters and some other microfossils related to recent coccolithophores. *J. Paleontol*. **28**, 385–403.
40. Goto T. 2001 Comparative anatomy, phylogeny, and cladistic classification of the order Orectolobiformes (Chondrichthyes, Elasmobranchii). *Memoirs Grad. Sch. Fish. Sci. Hokkaido Univ*. **48**, 1–100.
41. Swofford DL. 2003 *PAUP*. phylogenetic analysis using parsimony (*and other methods)*, 4th edn. Sunderland, Massachusetts: Sinauer Associates.
42. Ronquist F *et al*. 2012 MrBayes 3.2: efficient Bayesian phylogenetic inference and model choice across a large model space. *Syst. Biol*. **61**, 539–542. (doi:10.1093/sysbio/sys029)

43. Rambaut A, Drummond AJ, Xie D, Baele G, Suchard MA. 2018 Posterior summarization in Bayesian phylogenetics using Tracer 1.7. *Syst. Biol*. **67**, 901–904. (doi:10.1093/sysbio/syy032)
44. Paradis E, Schliep K. 2019 Ape 5.0: an environment for modern phylogenetics and evolutionary analyses in R. *Bioinformatics* **35**, 526–528. (doi:10.1093/bioinformatics/bty633)
45. Cappetta H. 1987 *Handbook of paleoichthyology. Volume 3B. Chondrichthyes ii. Mesozoic and Cenozoic Elasmobranchii*. (ed. H-P Schultze). Munich, Germany: Verlag Dr. Friedrich Pfeil.
46. Cappetta H. 2012 *Handbook of Paleoichthyology. volume 3E. Chondrichthyes. Mesozoic and Cenozoic Elasmobranchii: teeth*. (ed. H-P Schultze). Munich, Germany: Verlag Dr. Friedrich Pfeil.
47. Ridewood WG. 1921 On the calcification of the vertebral centra in sharks and rays. *Phil. Trans. R. Soc. B Contain. Pap. Biol. Character* **210**, 311–407.
48. White EG. 1937 Interrelationships of the elasmobranchs with a key to the order Galea. *Bull. Am. Mus. Nat. Hist.* **74**, 25–138. http://www.digitallibrary.amnh.org/handle/2246/369
49. Naylor GJP, Caira J, Jensen K, Rosana K, Straube N, Lakner C. 2012 Elasmobranch phylogeny: a mitochondrial estimate based on 595 species. In *Biology of sharks and their relatives* (eds JC Carrier, JA Musick, MR Heithaus), pp. 31–56. Oxford: CRC Press. (doi:10.1201/b11867-4)
50. Cappetta H. 1980 Les sélaciens du Crétacé supérieur du Liban. I: requins. *Palaeontogr. Abt*. **168**, 69–148.
51. Adnet S. 2006 Nouvelles faunes de sélaciens (Elasmobranchii, Neoselachii) de l'Eocène moyen des Landes (Sud—Ouest, France). Implication dans la connaissance des communautés de sélaciens d'eaux profondes. *Palaeo Ichthyol*. **10**, 5–128.
52. Cappetta H. 1976 Sélaciens nouveaux du London Clay de l'Essex (Yprésien du bassin de Londres). *Geobios* **9**, 551–575. (doi:10.1016/s0016-6995(76)80024-1)
53. Herman J. 1977 Les sélaciens des terrains néocrétacés et paléogènes de belgique et des contrées limitrophes. Eléments d'une biostratigraphie intercontinentale. *Mémoires Pour Servir à l'Explication Des Cartes Géologiques et Minières de La Belgique* **15**.
54. Underwood CJ, Mitchell S. 1999 Albian and Cenomanian (Late Cretaceous) selachian faunas from North East England. *Spec. Pap. Palaeontol*. **60**, 9–59.
55. Ebert DA, Fowler S, Compagno LJV. 2013 *Sharks of the world. a fully illustrated guide*. Plymouth, UK: Wild Nature Press.
56. Rees J. 2010 Neoselachian sharks from the Callovian-Oxfordian (Jurassic) of Ogrodzieniec, Zawiercie Region, southern Poland. *Palaeontology* **53**, 887–902. (doi:10.1111/j.1475-4983.2010.00967.x)
57. Srdic A, Duffin CJ, Martill DM. 2016 First occurrence of the orectolobiform shark *Akaimia* in the Oxford Clay Formation (Jurassic, Callovian) of England. *Proc. Geol. Assoc*. **127**, 506–513. (doi:10.1016/j.pgeola.2016.07.002)
58. Kriwet J. 2005 A Late Jurassic carpetshark (Neoselachii, Orectolobiformes) from southern Germany. In *Mesozoic fishes 4 – homology and phylogeny* (eds G Arratia, HP Schultze, MVH Wilson), pp. 443–454. München, Germany: Verlag Dr. Friedrich Pfeil.
59. Delsate D. 2003 Une nouvelle faune de poissons et requins toarciens du Sud du Luxembourg (Dudelange) et de l'Allemagne (Schömberg). *Bull. De L'Académie Lorraine Des Sci*.
60. Delsate D, Thies D. 1994 Teeth of the fossil shark *Annea* Thies 1983 (Elasmobranchii, Neoselachii) from the Toarcian of Belgium. *Belgian Geological Survey. Professional Paper* **278**, 45–64.
61. Kriwet J. 2003 Neoselachian remains (Chondrichthyes, Elasmobranchii) from the Middle Jurassic of SW Germany and NW Poland. *Acta Palaeontol. Pol.* **48**, 583–594.
62. Parham JF *et al*. 2012 Best practices for justifying fossil calibrations. *Syst. Biol*. **61**, 346–359. (doi:10.1093/sysbio/syr107)
63. Knaub JL, Passerotti M, Natanson LJ, Meredith T, Porter M. 2024 Vertebral morphology in the tail-whipping common thresher shark, *Alopias vulpinus*. *R. Soc. Open Sci*. **11**, 231473. (doi:10.1098/rsos.231473)
64. Kriwet J, Klug S, Canudo JI, Cuenca-bescos G. 2008 A new early Cretaceous lamniform shark (Chondrichthyes, Neoselachii). *Zool. J. Linn. Soc*. **154**, 278–290. (doi:10.1111/j.1096-3642.2008.00410.x)
65. Rees J. 2005 Neoselachian shark and ray teeth from the Valanginian, Lower Cretaceous, of Wawal, central Poland. *Palaeontology* **48**, 209–221. (doi:10.1111/j.1475-4983.2005.00441.x)
66. Dudgeon CL, Corrigan S, Yang L, Allen GR, Erdmann MV, Sugeha HY, White WT, Naylor GJP. 2020 Walking, swimming or hitching a ride? Phylogenetics and biogeography of the walking shark genus Hemiscyllium. *Mar. Freshwater Res*. **71**, 1107–1117. (doi:10.1071/MF19163)
67. Goto T, Last PR. 2001 A new parascyliid species, *Parascyllium sparsimaculatum*, from Western Australia (Elasmobranchii, Orectolobiformes). *Ichthyological Research*
68. Goto T, Nakaya K. 1996 Revision of the genus *Cirrhoscyllium*, with the designation of a neotype for C. *Jpn. Ichthyol*. (doi:10.1007/BF02347592)
69. Renema W *et al*. 2008 Hopping hotspots: global shifts in marine biodiversity. *Science* **321**, 654–657. (doi:10.1126/science.1155674)
70. Beckett H, Giles S, Friedman M. 2018 Comparative anatomy of the gill skeleton of fossil Aulopiformes (Teleostei: Eurypterygii). *J. Syst. Palaeontol*. **16**, 1221–1245. (doi:10.1080/14772019.2017.1387184)
71. Sendell-Price AT *et al*. 2023 Low mutation rate in epaulette sharks is consistent with a slow rate of evolution in sharks. *Nat. Commun*. **14**. (doi:10.1038/s41467-023-42238-x)
72. Dearden R, Johanson Z, O'Neill H *et al*. 2025 Data for: Three-dimensional fossils of a Cretaceous collared carpet shark (Parascylliidae, Orectolobiformes) shed light on skeletal evolution in galeomorphs [Dataset]. Dryad (doi:10.5061/dryad.n5tb2rc5r)
73. Dearden RP, Johanson Z, O'Neill HL, Miles K, Bernard EL, Clark B *et al*. 2025. Supplementary Material from: Three-Dimensional Fossils of a Cretaceous Collared Carpet Shark (Parascylliidae, Orectolobiformes) Shed Light on Skeletal Evolution in Galeomorphs. FigShare (doi:10.6084/m9.figshare.c.7778783)